CA9600671

AECL EACL

AECL-11190, COG-94-493

Moisture Distribution Computed from Electrical Impedance Tomographic Data of a Bentonite Clay/Sand Material

Distribution hygrométrique calculée à partir de données tomographiques d'impédance électrique d'un matériau composé d'argile bentonitique et de sable

Guye Stephenson Strobel

November 1995 novembre

AECL-11190
COG-94-493

MOISTURE DISTRIBUTION COMPUTED FROM ELECTRICAL-IMPEDANCE TOMOGRAPHIC DATA OF A BENTONITE CLAY/SAND MATERIAL

by

Guye Stephenson Strobel

Geotechnical Science and Engineering Branch
Whiteshell Laboratories
Pinawa, Manitoba R0E 1L0
1995

AECL-11190
COG-94-493

MOISTURE DISTRIBUTION COMPUTED FROM ELECTRICAL-IMPEDANCE TOMOGRAPHIC DATA OF A BENTONITE CLAY/SAND MATERIAL

by

Guye Stephenson Strobel

ABSTRACT

Moisture content values were calculated from electrical impedance-computed tomography measurements and compared with thermocouple psychrometer moisture values. The measurements were taken, *in situ* and under isothermal conditions, in a bentonite clay/sand packed borehole at the Underground Research Laboratory. Two sets of impedances moisture contents were calculated from the impedance values—independent of each other. For one set, impedance measurements were fitted to the psychrometer moisture values in a least-squares fit to a generalized calibration curve and, for the second set, an impedance-moisture relationship from laboratory calibrations was applied. The impedance-computed moisture content data showed low scatter and the trends were consistent between the three sets of values. However, the moisture content data computed from the calibration curve were more consistent with those expected from physical arguments. The moisture values from the psychrometer readings were offset and, consequently, so were those produced after applying the fitting strategy. Internal redistribution of moisture appears to have had a more significant effect on the system than did inflow at the boundary. Inflow did cause a significant change but this was localized, during this period, to the outer ~ 0.05 m of the test hole. No comment was made as to what internal processes caused these responses.

Geotechnical Science and Engineering Branch
Whiteshell Laboratories
Pinawa, Manitoba R0E 1L0
1995

AECL-11190
COG-94-493

DISTRIBUTION HYGROMÉTRIQUE CALCULÉE À PARTIR DE DONNÉES TOMOGRAPHIQUES D'IMPÉDANCE ÉLECTRIQUE D'UN MATÉRIAU COMPOSÉ D'ARGILE BENTONITIQUE ET DE SABLE

par

Guye Stephenson Strobel

RÉSUMÉ

Les valeurs de la teneur en humidité ont été calculées à partir de mesures de tomographie établies par impédance électrique et comparées aux valeurs obtenues à l'aide d'un micropsychromètre. Les mesures ont été prises *in situ* et dans des conditions isothermes, au Laboratoire de recherches souterrain, dans un trou de forage comblé d'argile bentonitique et de sable. Deux séries indépendantes l'une de l'autre des teneurs en humidité liées aux impédances ont été calculées à partir des valeurs d'impédance. Dans la première série, on a adapté les mesures d'impédance aux valeurs d'humidité relevées par le micropsychromètre par ajustement des moindres carrés à une courbe d'étalonnage généralisée et, dans la seconde, on a appliqué une relation impédance-humidité provenant des étalonnages réalisés en laboratoire. Les données sur la teneur en humidité calculée par impédance présentaient une faible dispersion, et les tendances parmi les trois séries de valeurs étaient cohérentes. Toutefois, les données de la teneur en humidité calculée à partir de la courbe d'étalonnage concordaient mieux avec celles auxquelles on pouvait s'attendre en s'appuyant sur des arguments physiques. Les valeurs de l'humidité relevées par le micropsychromètre étaient décalées et, en conséquence, celles fournies après l'application de la méthode d'ajustement l'étaient également. La redistribution interne de l'humidité semble avoir eu beaucoup plus d'effet sur le système que n'en a eu l'afflux d'eau à la frontière. L'entrée d'eau a été en fait à l'origine d'une modification importante, quoique restreinte, durant cette période, à ~ 0,05 m de la périphérie du forage d'essai. Aucune explication des processus internes ayant provoqué ces réactions n'a été formulée.

Sciences et études géotechniques
Laboratoires de Whiteshell
Pinawa (Manitoba) R0E 1L0
1995

CONTENTS

		Page
1.	INTRODUCTION	1
2.	PURPOSE	1
3.	METHOD	1
4.	RESULTS	3
5.	DISCUSSION	4
6.	CONCLUSIONS	6
ACKNOWLEDGMENTS		6

1. INTRODUCTION

This report compares *in situ* moisture content values calculated from conductances computed using electrical impedance-computed tomography (EICT) data, with moisture values computed from psychrometer measurements. The measurements were made in a bentonite clay/sand material (buffer) comprising 50% bentonite clay and 50% sand. Electrical impedance measurements have been shown to vary with moisture content (Strobel 1994c) and an understanding of the behavior of moisture is important in assessing the performance of clay-based barriers proposed within the disposal concept. The tests were conducted at the Underground Research Laboratory (URL) as part of Canada's Nuclear-Fuel Waste Management Program (NFWMP) (Dormuth and Gillespie 1990).

To make this comparison, two different moisture calibrations were applied to the EICT data. One set of moisture content values were derived from a least-squares fit to a general form for the calibration curve using independently determined psychrometer moisture content values (Strobel 1994b) (referred to as the "*in situ* calibration".) The second set was derived from a calibration curve calculated from laboratory measurements on samples of known moisture content (referred to as the "laboratory calibration".)

2. PURPOSE

The purpose of this study was to compare moisture contents computed from conductance values from EICT measurements made on buffer with independent moisture content calculations from psychrometer(Wan 1995) readings. Point measurements of water content were made using thermocouple psychrometers in conjunction with EICT monitoring, over the four-month period reported here, beginning in December of 1992.

3. METHOD

All measurements used in this analysis were taken in a 0.624-m-radius, borehole packed with two meters of buffer and capped with a 1.25-m concrete plug (Strobel 1995). The borehole was drilled into the rock floor on the 240 *Level* of the Underground Research Laboratory (Simmons 1987) in Lac du Bonnet, Manitoba. Figure 6.1 shows the apparatus and location of the electrodes used for the tests. The electrodes were 1 – m–long wires, installed vertically and arranged evenly around the rock walls of the borehole starting 0.5 m from the bottom. A 10 mA direct-current source was used for excitation while voltage measurements were made around the outer wall of the borehole (Strobel 1995).

The EICT results were continuous functions representing horizontal cross-sections of the buffer conductance. Line electrodes were used to vertically average the readings over the length of the electrodes. The psychrometer measurements were made along two horizontal profiles at right-angles to each other in a plane directly above the EICT measurements. Six

such sensors were installed along a profile while four others were installed along a profile at right-angles to the first.

An empirical and general form of the calibration relationship (impedance versus moisture content) has been deduced from laboratory measurements (Strobel 1994c):

$$\rho = a + b\exp(-M/c) \tag{3.1}$$

where

- $\rho \propto C^{-1} \equiv$ resistivity (Ωm)
- $C \equiv$ conductivity (S)
- $M \equiv$ moisture content (%)
- a, b, c are parameters of the calibration curve

Equation 3.1 is equivalent to the empirical formula due to Archie (Archie 1942), describing the relationship between moisture content and resistivity (ρ_e) for a porous material

$$\rho_e = \mu\phi^{-M}s^{-n}\rho_w \tag{3.2}$$

where ϕ = porosity, s = fraction of the pores containing water, ρ_w = resistivity of water, $n \approx 2$ and μ, M are constants. Equation 3.1 is equivalent to Equation 3.2 with a zero and, from Equation 3.2:

$$\rho_e = \xi(\tau\epsilon)^M$$

where $\xi \equiv \mu s^{-n}\rho_w$, and $\tau\epsilon \equiv \phi$. Equating $(\tau\epsilon)^{-M}$ to $e^{-M/c}$ yields

$$c = ln^{-1}(\tau\epsilon)$$

Equation 3.1 can be solved for moisture content (M) in terms of the conductance (C):

$$M = \alpha - \beta\ln(1/C - a) \tag{3.3}$$

Rewriting Equation 3.3 gives:

$$M = \alpha - \beta\ln[1/C(1 - Ca)]$$

where

- $\alpha = c\ln b$
- $\beta = c$

If C is small compared to a (ie., $1/C \gg a$), then Equation 3.3 reduces to

$$M = \alpha + \beta \ln C \tag{3.4}$$

In addition to calibrating the results (Equation 3.4), the general form of Equation 3.4 was fitted to the psychrometer data using a least-squares method(Strobel 1994b). The *in situ* calibration assumed the psychrometer moisture content values were accurate to derive the values of α and β. For these comparisons, all data was used within $\pm 5°$ of the profile defined by the positioning of the psychrometer sensors.

4. RESULTS

Since EICT conductance measurements were of the order of $10^{-4}(S)$, whereas the value of a is of order 10^0, the reduced form for the calibration curve (Equation 3.4) holds.

The resistivity-moisture content curve derived from laboratory measurements was calibrated using *in situ* thermocouple psychrometer readings to determine the parameters (α and β) of the calibration curve. To make the laboratory resistance measurements consistent with the point-conductance measurements of the EICT study, the measured resistivity was divided by the measurement electrode separation to generate:

$$\partial R/\partial x = \triangle R/\triangle x$$

where

$$\partial R \equiv \partial V/I$$

and where $\triangle x$ is the measurement electrode separation and the current (I) is constant. Resistivity is a calculation from a voltage measurement done to eliminate the effect of geometry: ie., although the voltage measured will depend on geometry, the resistivity will not.

The calibration voltage readings(Strobel 1994c) are included in Table 6.1. The factor used to multiply the measured voltage reading to obtain the point conductance (geometry independent) was

$$[\pi r^2]/[2d^2 I] = (\pi \times (0.05)^2)/(2 \times 0.01 \times 0.06^2)\ A^{-1} = 109.08\ A^{-1}$$

where $I = 0.010\ A$ was the current applied, $d \sim 60.0\ mm$ was the measurement electrode separation, and $r = 0.05\ mm$ the radius of the sample. The resultant values of a, b, and c in Equation 3.3, are 149.0 (Ω-m), 7.577×10^4 (Ω-m) and 2.687 (%) respectively. The factor of 1/2 is applied to average the voltage between the negative and positive polarity excitations. This calculation was done to eliminate the effect due to the spontaneous potential at the measurement electrodes. In the region of interest, moisture content of $\sim$ 18%, the ratio of the terms $a/[be^{[-M/c]}]$ is of the order 10^0. Equation 3.4 becomes:

$$M = 30.190 + 2.687 \ln C$$

The *in situ* calibration calculations were done using the 1993 February 6 data. The values for a and b are 29.515 (Ω-m) and 2.34 (Ω-m) respectively. The conductance measurements were converted to moisture content using both laboratory and *in situ* calibrations with the results contained in Table 6.2. The results were compared in Figure 6.2.

Figure 6.3 plots conductance moisture contents computed for several days data spread over approximately six months as differences using 1992 December 05 as the reference profile. This plot provides information on moisture inflow at the borehole wall. Here, the sharp discontinuity in the conductance has obscured the moisture results because the shape functions used for numerical solution of the conductances cannot accelerate fast enough to produce an accurate value.

5. DISCUSSION

Figure 6.4 shows that laboratory calibrated EICT moisture content values range around the expected emplacement level of ~ 18.0% at the beginning of the monitoring (Dixon, Campbell, and Hnatiw 1994).

The laboratory calibrations were performed at 1.67 Mg/m^3 whereas the preplaced buffer moisture was ~ 1.73 Mg/m^3 (Dixon, Campbell, and Hnatiw 1994). The higher emplacement density would manifest itself in a higher apparent moisture content but this correction is not insignificant in the range of conditions experienced. This is shown from the density-resistivity relationship which has the same form as the moisture content-resistivity relationship (Strobel 1994a), ie.,

$$\rho = a' + b' exp(-D/c') \tag{5.1}$$

where $a' = 1.42 \times 10^2$ (Ω-m), $b' = 6.74 \times 10^5$ (Ω-m), and $c' = 1.42 \times 10^{-1}$ ($[Mg/m^3]^{-1}$) were computed as above. From Equations 3.1 and 5.1

$$\delta\rho = (b'/c')\exp[-D/c']\delta D$$

and

$$\delta\rho = (b/c)\exp[-M/c]\delta M$$

Hence

$$\delta M/\delta D = (b'/b)(c/c')(\exp[M/c]\exp[-D/c']$$

Substituting the values of b, c, b', and c' into the above using $M = 17.5\%$ and $D = 1.71$ Mg/m^3:

$$\delta M/\delta D = 0.168\ \%/(Mg/m^3)$$

For a difference of 0.08 Mg/m^3, this translates into an apparent moisture content variation of 0.13%.

Fitting the EICT data to the psychrometer data for the *in situ* calibration implies that the psychrometer data is a measurement standard. Alternatively, evaluating the psychrometer results as compared to the EICT measurements helps to understand the performance of the

psychrometers. The trends in both data sets is consistent and this observation is validated by the other results (Strobel 1994b). However, the psychrometer and laboratory calibrated EICT results are offset relative to each other by ~ 10% of the readings. The psychrometer data is higher then expected: averaging 19 to 20% by mass from early in the tests when the expected results should be less then 18%. The consistency in the trends with the EICT results help validate the psychrometer moisture content trends, if not their absolute values. To make them consistent in magnitude they need only be linearly transformed. The fact that the parameters in the calibrated *in situ* relationship are close to those of the calibration curve, differing by $\ll 1\%$ and 13% for α and β respectively, implies that this shift is small. The transformation can be calculated from the calibration curves (above):

$$M = M'(\beta/\beta') + [\alpha - \beta/\beta'\alpha']$$

$$= 0.9776 \times M' - 0.278$$

where M is the corrected moisture content and M' is the calculated psychrometer moisture content. This is an offset of ~ 10% at 18% moisture content: consistent with the observed offset for the psychrometer values.

The expected inflow of moisture from the walls of the borehole is apparent from Figure 6.3 as an increase in moisture at the ends of the plot. The moisture levels computed for boundary will be lower than the actual moisture content because the analysis used nodes placed on the rock-buffer interface. The rock has a lower conductance than the buffer and the fit produced will be influenced by both the buffer and the rock.

The factors having the largest influence on the response of the system appears to be internal since the internal response is significantly greater than that caused by direct moisture inflow. Changes in moisture content of up to 2% in four months has affected all regions of the system. The magnitude of the moisture inflow cannot be directly determined from the EICT readings due to the effect of the rock wall: however, the change in moisture content can give this result. It appears that significant moisture inflows are occurring at the boundary, but, restricted to the outer 0.5 *m* of the borehole.

The result from calibration with laboratory measurements show a similar trend to the results from the *in situ* calibration. They are offset downwards. This consistency in the trend is not surprising since the form of the calibration curves used are the same with only the calibration parameters calculated in a different manner. The results from the laboratory calibration were more consistent with the preplaced moisture of the buffer. The distributed change in the moisture content for 1993 February 6 is displayed in Figure 6.5.

Equation 3.2 assumes the electrical resistivity of the buffer is dominated by the pore water. If this is the case, the results of these tests can be used to deduce a value for the porosity of the *in situ* buffer. That the parameter a in Equation 3.1 is not insignificant suggests there is a major contribution to the resistivity due to the buffer matrix. This would be the contribution due to the clay minerals. Considering the second term in Equation 3.1 to be due to the pore water: since $\phi = \xi\epsilon$ and $c = ln^{-1}(\xi\epsilon)$, then the porosity (void volume/total volume) of the *in situ* buffer is $\phi = \epsilon^{[-1/c]} = 0.652$. This value is high compared to the expected ~ 0.40 (D.

Dixon, personal communication) which could be due to the high clay content of the buffer causing a lower resistivity.

6. CONCLUSIONS

The results show that the EICT method can be used to monitor buffer to produce a quantitative result for moisture distribution. The trend in these results were validated by the psychrometer readings. The EICT and psychrometer moisture values were offset relative to each other; however, independently calibrated EICT moisture values were consistent with the initial conditions of the system. The absolute results for the EICT moisture values are incorrect at the boundary of the system because the electrodes were placed on the buffer-rock interface. The interface is a mathematical discontinuity for the processing model and the conductance of the associated nodes will not be able to determine a correct value at these nodes. However, by presenting the data as a change relative to a reference date, as in Figure 6.5, a change in moisture content can be calculated for this region.

ACKNOWLEDGMENTS

The Canadian Nuclear Fuel Waste Management Program is jointly funded by AECL and Ontario Hydro under the auspices of the CANDU Owners Group.

REFERENCES

Archie, G. 1942. The electrical resistivity log as an aid in determining some reservoir characteristics. Trans. A.I.M.E. 146, 54-62.

Dixon, D., S. Campbell, and D. Hnatiw. 1994. Preplacement quality control and as-placed properties of the buffer materials used in the URL Isothermal Buffer Experiment. Atomic Energy of Canada Limited, Technical Record TR-612, COG-94-35.

Dormuth, K. and P. Gillespie. 1990. Nuclear fuel waste disposal in Canada—the generic research program. Atomic Energy of Canada Limited, Technical Report AECL-10183.

Simmons, G. 1987. Atomic Energy of Canada Limited's Underground Research Laboratory for Nuclear Waste Management. Atomic Energy of Canada Limited, Technical Report AECL-9283.

Strobel, G. 1994a. Measurements of resistive and capacitive properties of a sand/bentonite clay mixture. Atomic Energy of Canada Limited, Technical Report AECL-10668, COG-92-195.

Strobel, G. 1994b. A method for fitting multiple sets of noncoincidental stochastic data. Atomic Energy of Canada Limited, Technical Report TR-450, COG-94-468.

Strobel, G. 1994c. Resistivity-water content relationship of a sand/bentonite clay mixture. Atomic Energy of Canada Limited, Technical Report TR-600, COG-93-90.

Strobel, G. 1995. An impedance-computed tomographic data acquisition system. Atomic Energy of Canada Limited, Technical report.

Van, A. 1995. An appraisal of the usefulness and limitations of commercial thermocouple psychrometers for soil suction potential measurements. Atomic Energy of Canada Limited, Technical Report AECL-11091.

TABLE 6.1:

Laboratory Data Determining Calibration Curve

Moisture Content (%)	Measured Voltage (V)	Point Resistance (Ω)
14.86	4.088	445.58
15.44	3.3586	366.37
15.52	3.6306	396.04
15.99	3.2525	354.79
16.40	3.1088	339.12
16.78	2.8324	308.97
17.60	2.3404	263.98
17.61	2.2778	255.30
17.50	2.420	248.47
17.99	2.3296	254.12
18.07	1.9994	218.10
18.31	2.1644	236.10
18.40	2.0892	227.96
18.57	1.8898	206.15
19.64	1.8238	198.95
19.69	1.7678	192.84
20.33	1.6966	185.07
20.46	1.6642	181.54
21.79	1.6384	175.91
21.73	1.6126	178.72
21.83	1.6696	182.13

TABLE 6.2:

In Situ and Laboratory Calibrated Moisture Contents

Distance from center (m)	Laboratory Calibrated Moisture (%)	Calibrated *in situ* Moisture (%)	Distance from center (m)	Laboratory Calibrated Moisture (%)	Calibrated *in situ* Moisture (%)
-0.611	15.55	17.17	0.113	18.41	19.66
-0.611	15.67	17.27	0.141	18.52	19.75
-0.611	15.43	17.07	0.190	18.59	19.82
-0.566	15.81	17.40	0.239	18.63	19.85
-0.566	15.70	17.30	0.267	18.49	19.73
-0.566	15.67	17.27	0.316	18.33	19.59
-0.522	16.16	17.70	0.359	17.99	19.29
-0.522	16.27	17.79	0.365	17.87	19.19
-0.522	16.17	17.71	0.388	17.85	19.17
-0.494	16.18	17.72	0.394	17.64	18.98
-0.493	16.47	17.97	0.440	16.67	18.14
-0.443	17.16	18.57	0.443	16.61	18.09
-0.440	17.10	18.51	0.493	15.88	17.46
-0.394	17.70	19.04	0.494	15.72	17.32
-0.388	17.67	19.01	0.522	15.58	17.20
-0.365	17.96	19.27	0.522	15.57	17.19
-0.359	17.74	19.07	0.522	15.52	17.14
-0.316	18.21	19.48	0.566	15.12	16.80
-0.267	18.20	19.48	0.566	15.13	16.80
-0.239	18.26	19.53	0.566	15.11	16.79
-0.190	18.14	19.42	0.611	14.88	16.58
-0.141	17.91	19.22	0.611	15.06	16.74
-0.113	17.92	19.23	0.611	15.12	16.80

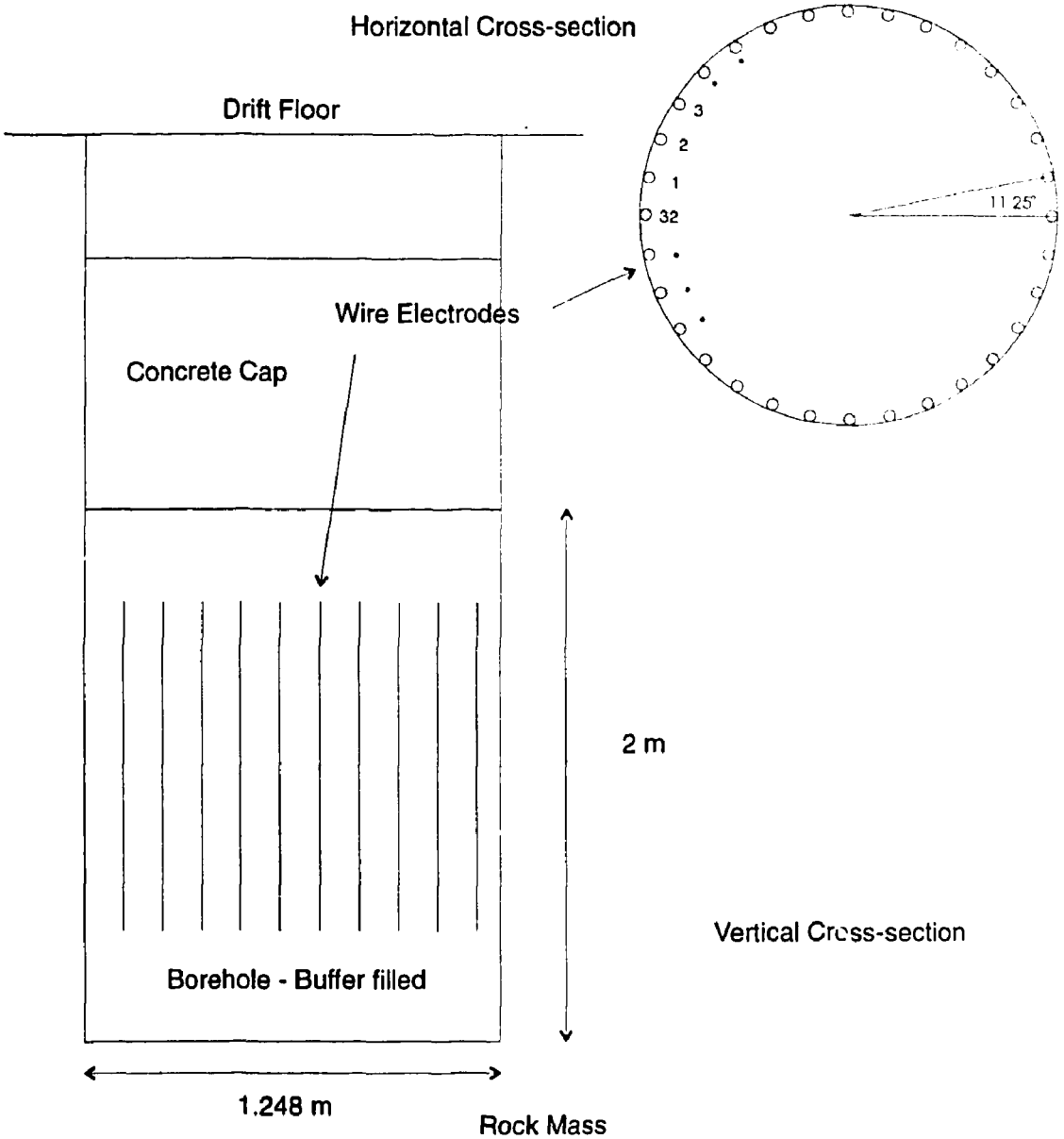

FIGURE 6.1: Apparatus used for the Reported Tests. The electrodes were installed in a borehole in the floor of the drift and selected in pairs for the excitation circuit. Voltages were measured at the other electrodes.

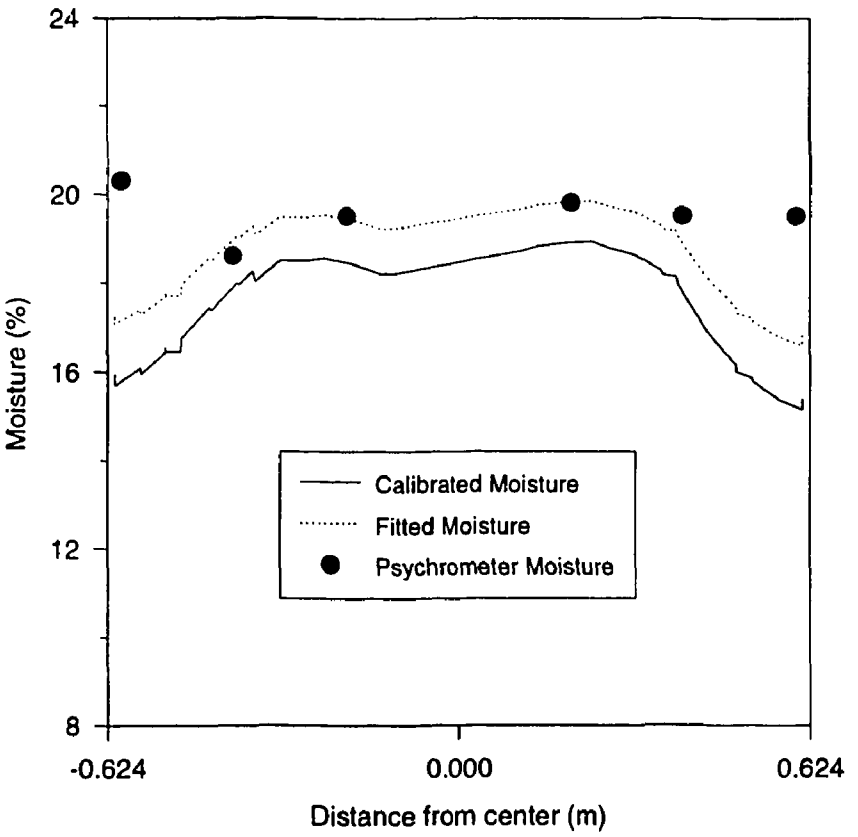

FIGURE 6.2: Plot of Fitted and Laboratory Calibrated Data for 1993 February 6. The conductance data was calibrated using the results of (Strobel 1994c) and, alternatively, fitted according to (Strobel 1994b). The average moisture content is computed from moisture distributions (Dixon, Campbell, and Hnatiw 1994) in the buffer in the $1 - m$ region surrounded by the electrodes. The psychrometer readings were also plotted.

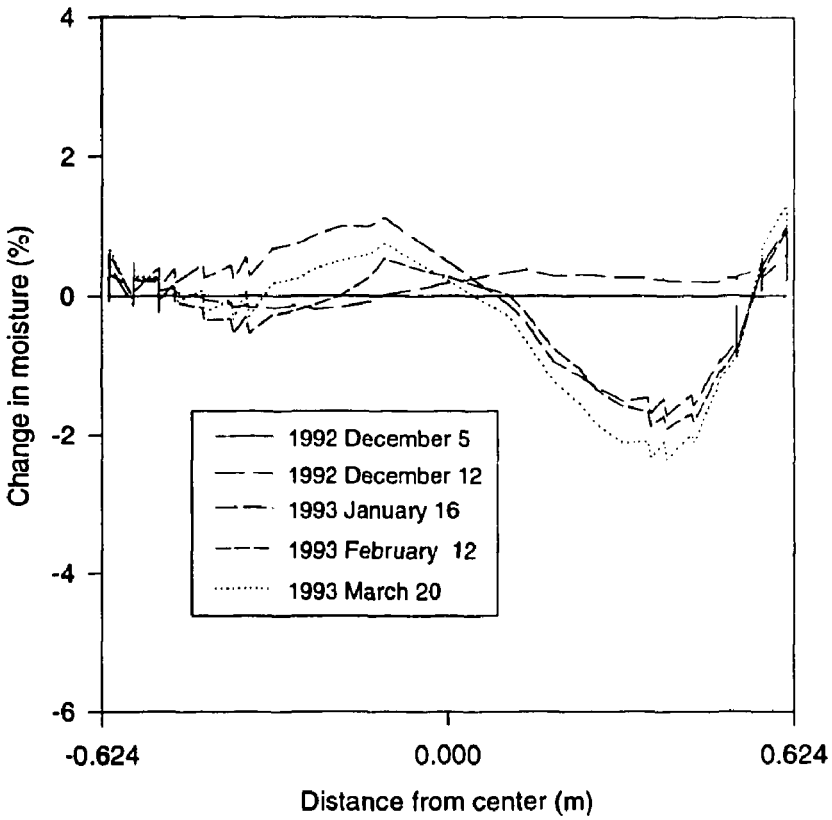

FIGURE 6.3: Change in Moisture Content over Four Months. The moisture content was computed from the calibration curve for measurements and the profiles were plotted for four days over four months. The reference profile used was 1992 December 5.

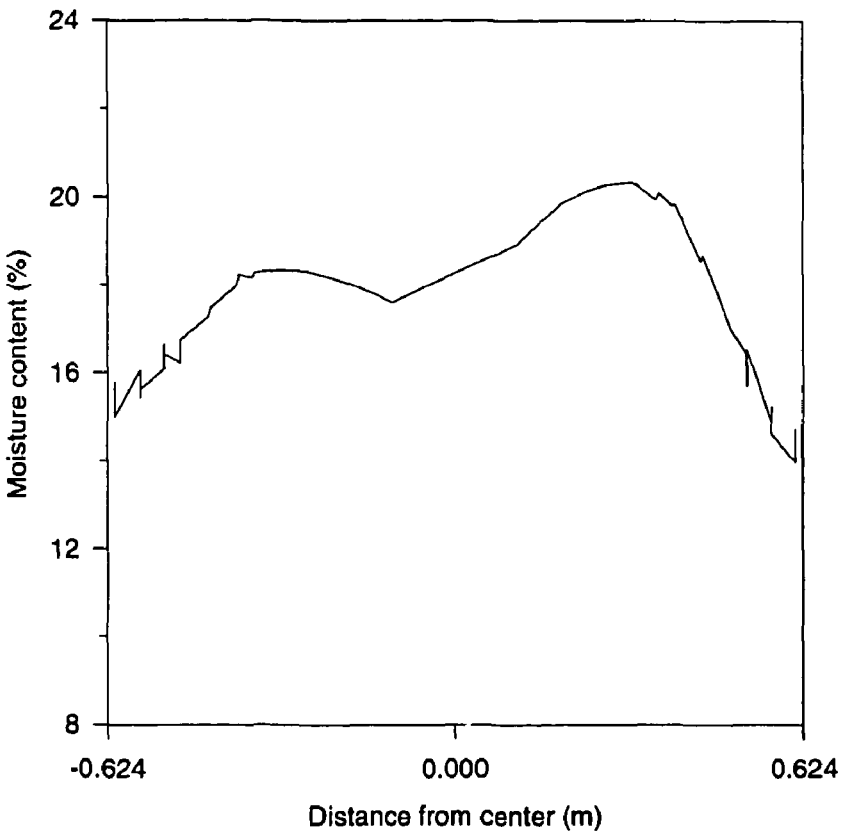

FIGURE 6.4: Laboratory Calibrated Data for 1992 December 5. The conductance data determined from the EICT survey was calibrated using results from the laboratory tests.

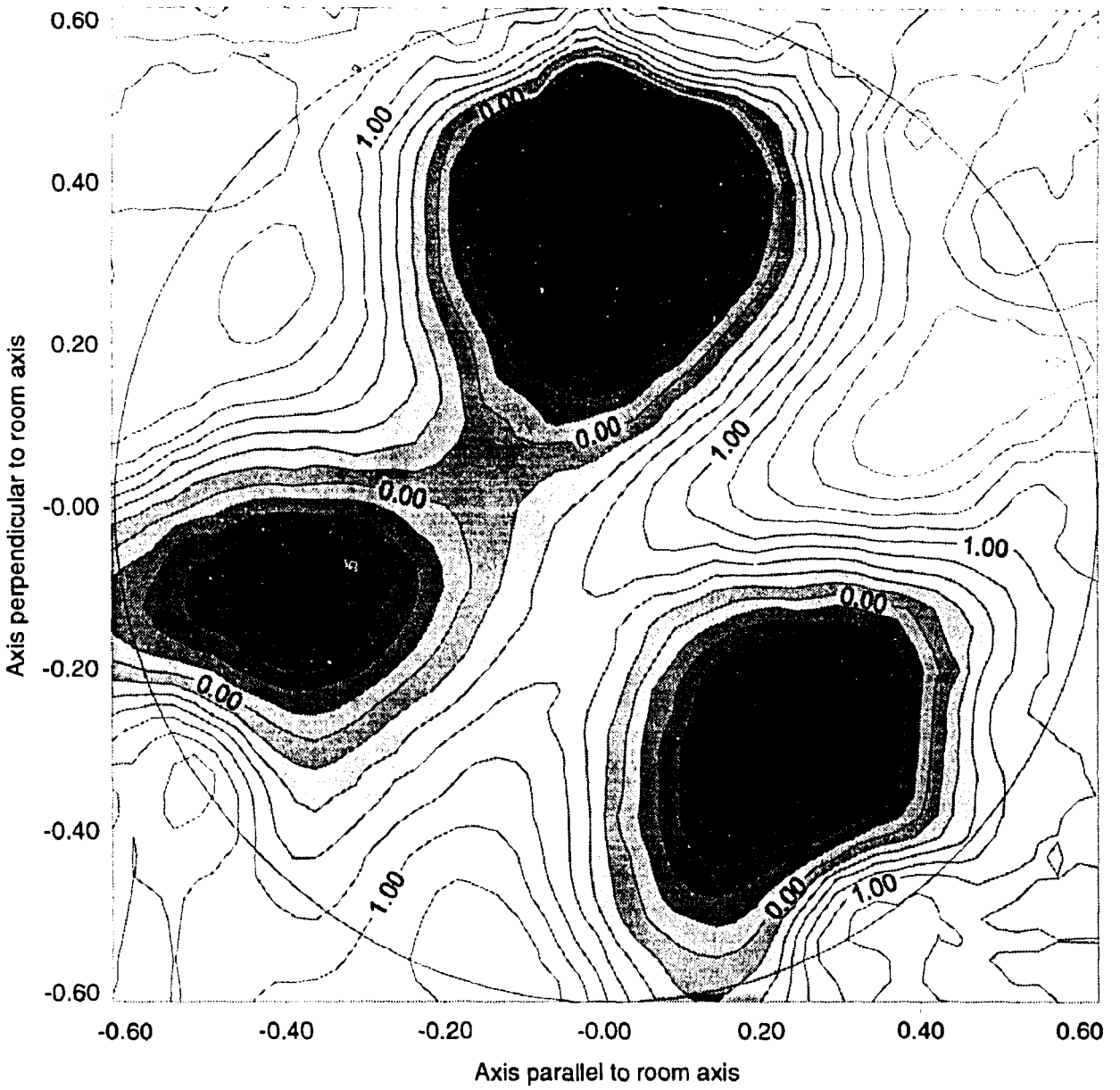

FIGURE 6.5: Moisture Plot from Laboratory Calibrated Conductance Readings. The plot is a distribution of the change in moisture content as of 1993 February 06, relative to 1992 December 05. Units are % moisture content.

Cat. No. / Nº de cat.: CC2-11190E
ISBN 0-660-16274-8
ISSN 0067-0367

To identify individual documents in the series, we have assigned an AECL- number to each. Please refer to the AECL- number when requesting additional copies of this document from

Scientific Document Distribution Office (SDDO)
AECL
Chalk River, Ontario
Canada K0J 1J0

Fax: (613) 584-1745 Tel.: (613) 584-3311
ext. 4623

Price: A

Pour identifier les rapports individuels faisant partie de cette série, nous avons affecté un numéro AECL- à chacun d'eux. Veuillez indiquer le numéro AECL- lorsque vous demandez d'autres exemplaires de ce rapport au

Service de Distribution des documents officiels (SDDO)
EACL
Chalk River (Ontario)
Canada K0J 1J0

Fax: (613) 584-1745 Tél.: (613) 584-3311
poste 4623

Prix: A

CA9600671

AECL EACL

AECL-11190, COG-94-493

Moisture Distribution Computed from Electrical Impedance Tomographic Data of a Bentonite Clay/Sand Material

Distribution hygrométrique calculée à partir de données tomographiques d'impédance électrique d'un matériau composé d'argile bentonitique et de sable

Guye Stephenson Strobel

November 1995 novembre

AECL-11190
COG-94-493

MOISTURE DISTRIBUTION COMPUTED FROM ELECTRICAL-IMPEDANCE TOMOGRAPHIC DATA OF A BENTONITE CLAY/SAND MATERIAL

by

Guye Stephenson Strobel

Geotechnical Science and Engineering Branch
Whiteshell Laboratories
Pinawa, Manitoba R0E 1L0
1995

AECL-11190
COG-94-493

MOISTURE DISTRIBUTION COMPUTED FROM ELECTRICAL-IMPEDANCE TOMOGRAPHIC DATA OF A BENTONITE CLAY/SAND MATERIAL

by

Guye Stephenson Strobel

ABSTRACT

Moisture content values were calculated from electrical impedance-computed tomography measurements and compared with thermocouple psychrometer moisture values. The measurements were taken, *in situ* and under isothermal conditions, in a bentonite clay/sand packed borehole at the Underground Research Laboratory. Two sets of impedances moisture contents were calculated from the impedance values—independent of each other. For one set, impedance measurements were fitted to the psychrometer moisture values in a least-squares fit to a generalized calibration curve and, for the second set, an impedance-moisture relationship from laboratory calibrations was applied. The impedance-computed moisture content data showed low scatter and the trends were consistent between the three sets of values. However, the moisture content data computed from the calibration curve were more consistent with those expected from physical arguments. The moisture values from the psychrometer readings were offset and, consequently, so were those produced after applying the fitting strategy. Internal redistribution of moisture appears to have had a more significant effect on the system than did inflow at the boundary. Inflow did cause a significant change but this was localized, during this period, to the outer ~ 0.05 m of the test hole. No comment was made as to what internal processes caused these responses.

Geotechnical Science and Engineering Branch
Whiteshell Laboratories
Pinawa, Manitoba R0E 1L0
1995

AECL-11190
COG-94-493

DISTRIBUTION HYGROMÉTRIQUE CALCULÉE À PARTIR DE DONNÉES TOMOGRAPHIQUES D'IMPÉDANCE ÉLECTRIQUE D'UN MATÉRIAU COMPOSÉ D'ARGILE BENTONITIQUE ET DE SABLE

par

Guye Stephenson Strobel

RÉSUMÉ

Les valeurs de la teneur en humidité ont été calculées à partir de mesures de tomographie établies par impédance électrique et comparées aux valeurs obtenues à l'aide d'un micropsychromètre. Les mesures ont été prises *in situ* et dans des conditions isothermes, au Laboratoire de recherches souterrain, dans un trou de forage comblé d'argile bentonitique et de sable. Deux séries indépendantes l'une de l'autre des teneurs en humidité liées aux impédances ont été calculées à partir des valeurs d'impédance. Dans la première série, on a adapté les mesures d'impédance aux valeurs d'humidité relevées par le micropsychromètre par ajustement des moindres carrés à une courbe d'étalonnage généralisée et, dans la seconde, on a appliqué une relation impédance-humidité provenant des étalonnages réalisés en laboratoire. Les données sur la teneur en humidité calculée par impédance présentaient une faible dispersion, et les tendances parmi les trois séries de valeurs étaient cohérentes. Toutefois, les données de la teneur en humidité calculée à partir de la courbe d'étalonnage concordaient mieux avec celles auxquelles on pouvait s'attendre en s'appuyant sur des arguments physiques. Les valeurs de l'humidité relevées par le micropsychromètre étaient décalées et, en conséquence, celles fournies après l'application de la méthode d'ajustement l'étaient également. La redistribution interne de l'humidité semble avoir eu beaucoup plus d'effet sur le système que n'en a eu l'afflux d'eau à la frontière. L'entrée d'eau a été en fait à l'origine d'une modification importante, quoique restreinte, durant cette période, à ~ 0,05 m de la périphérie du forage d'essai. Aucune explication des processus internes ayant provoqué ces réactions n'a été formulée.

Sciences et études géotechniques
Laboratoires de Whiteshell
Pinawa (Manitoba) R0E 1L0
1995

CONTENTS

		Page
1.	INTRODUCTION	1
2.	PURPOSE	1
3.	METHOD	1
4.	RESULTS	3
5.	DISCUSSION	4
6.	CONCLUSIONS	6
ACKNOWLEDGMENTS		6

1. INTRODUCTION

This report compares *in situ* moisture content values calculated from conductances computed using electrical impedance-computed tomography (EICT) data, with moisture values computed from psychrometer measurements. The measurements were made in a bentonite clay/sand material (buffer) comprising 50% bentonite clay and 50% sand. Electrical impedance measurements have been shown to vary with moisture content (Strobel 1994c) and an understanding of the behavior of moisture is important in assessing the performance of clay-based barriers proposed within the disposal concept. The tests were conducted at the Underground Research Laboratory (URL) as part of Canada's Nuclear-Fuel Waste Management Program (NFWMP) (Dormuth and Gillespie 1990).

To make this comparison, two different moisture calibrations were applied to the EICT data. One set of moisture content values were derived from a least-squares fit to a general form for the calibration curve using independently determined psychrometer moisture content values (Strobel 1994b) (referred to as the "*in situ* calibration".) The second set was derived from a calibration curve calculated from laboratory measurements on samples of known moisture content (referred to as the "laboratory calibration".)

2. PURPOSE

The purpose of this study was to compare moisture contents computed from conductance values from EICT measurements made on buffer with independent moisture content calculations from psychrometer(Wan 1995) readings. Point measurements of water content were made using thermocouple psychrometers in conjunction with EICT monitoring, over the four-month period reported here, beginning in December of 1992.

3. METHOD

All measurements used in this analysis were taken in a 0.624-m-radius, borehole packed with two meters of buffer and capped with a 1.25-m concrete plug (Strobel 1995). The borehole was drilled into the rock floor on the 240 *Level* of the Underground Research Laboratory (Simmons 1987) in Lac du Bonnet, Manitoba. Figure 6.1 shows the apparatus and location of the electrodes used for the tests. The electrodes were 1 – m–long wires, installed vertically and arranged evenly around the rock walls of the borehole starting 0.5 m from the bottom. A 10 mA direct-current source was used for excitation while voltage measurements were made around the outer wall of the borehole (Strobel 1995).

The EICT results were continuous functions representing horizontal cross-sections of the buffer conductance. Line electrodes were used to vertically average the readings over the length of the electrodes. The psychrometer measurements were made along two horizontal profiles at right-angles to each other in a plane directly above the EICT measurements. Six

such sensors were installed along a profile while four others were installed along a profile at right-angles to the first.

An empirical and general form of the calibration relationship (impedance versus moisture content) has been deduced from laboratory measurements (Strobel 1994c):

$$\rho = a + b\exp(-M/c) \tag{3.1}$$

where

- $\rho \propto C^{-1} \equiv$ resistivity (Ωm)
- $C \equiv$ conductivity (S)
- $M \equiv$ moisture content (%)
- a, b, c are parameters of the calibration curve

Equation 3.1 is equivalent to the empirical formula due to Archie (Archie 1942), describing the relationship between moisture content and resistivity (ρ_e) for a porous material

$$\rho_e = \mu\phi^{-M}s^{-n}\rho_w \tag{3.2}$$

where ϕ = porosity, s = fraction of the pores containing water, ρ_w = resistivity of water, $n \approx 2$ and μ, M are constants. Equation 3.1 is equivalent to Equation 3.2 with a zero and, from Equation 3.2:

$$\rho_e = \xi(\tau\epsilon)^M$$

where $\xi \equiv \mu s^{-n}\rho_w$, and $\tau\epsilon \equiv \phi$. Equating $(\tau\epsilon)^{-M}$ to $e^{-M/c}$ yields

$$c = ln^{-1}(\tau\epsilon)$$

Equation 3.1 can be solved for moisture content (M) in terms of the conductance (C):

$$M = \alpha - \beta\ln(1/C - a) \tag{3.3}$$

Rewriting Equation 3.3 gives:

$$M = \alpha - \beta\ln[1/C(1 - Ca)]$$

where

- $\alpha = c\ln b$
- $\beta = c$

If C is small compared to a (ie., $1/C \gg a$), then Equation 3.3 reduces to

$$M = \alpha + \beta \ln C \tag{3.4}$$

In addition to calibrating the results (Equation 3.4), the general form of Equation 3.4 was fitted to the psychrometer data using a least-squares method(Strobel 1994b). The *in situ* calibration assumed the psychrometer moisture content values were accurate to derive the values of α and β. For these comparisons, all data was used within $\pm 5°$ of the profile defined by the positioning of the psychrometer sensors.

4. RESULTS

Since EICT conductance measurements were of the order of $10^{-4}(S)$, whereas the value of a is of order 10^0, the reduced form for the calibration curve (Equation 3.4) holds.

The resistivity-moisture content curve derived from laboratory measurements was calibrated using *in situ* thermocouple psychrometer readings to determine the parameters (α and β) of the calibration curve. To make the laboratory resistance measurements consistent with the point-conductance measurements of the EICT study, the measured resistivity was divided by the measurement electrode separation to generate:

$$\partial R/\partial x = \triangle R/\triangle x$$

where

$$\partial R \equiv \partial V/I$$

and where $\triangle x$ is the measurement electrode separation and the current (I) is constant. Resistivity is a calculation from a voltage measurement done to eliminate the effect of geometry: ie., although the voltage measured will depend on geometry, the resistivity will not.

The calibration voltage readings(Strobel 1994c) are included in Table 6.1. The factor used to multiply the measured voltage reading to obtain the point conductance (geometry independent) was

$$[\pi r^2]/[2d^2 I] = (\pi \times (0.05)^2)/(2 \times 0.01 \times 0.06^2)\ A^{-1} = 109.08\ A^{-1}$$

where $I = 0.010\ A$ was the current applied, $d \sim 60.0\ mm$ was the measurement electrode separation, and $r = 0.05\ mm$ the radius of the sample. The resultant values of a, b, and c in Equation 3.3, are 149.0 (Ω-m), 7.577×10^4 (Ω-m) and 2.687 (%) respectively. The factor of 1/2 is applied to average the voltage between the negative and positive polarity excitations. This calculation was done to eliminate the effect due to the spontaneous potential at the measurement electrodes. In the region of interest, moisture content of $\sim$ 18%, the ratio of the terms $a/[be^{[-M/c]}]$ is of the order 10^0. Equation 3.4 becomes:

$$M = 30.190 + 2.687 \ln C$$

The *in situ* calibration calculations were done using the 1993 February 6 data. The values for a and b are 29.515 (Ω-m) and 2.34 (Ω-m) respectively. The conductance measurements were converted to moisture content using both laboratory and *in situ* calibrations with the results contained in Table 6.2. The results were compared in Figure 6.2.

Figure 6.3 plots conductance moisture contents computed for several days data spread over approximately six months as differences using 1992 December 05 as the reference profile. This plot provides information on moisture inflow at the borehole wall. Here, the sharp discontinuity in the conductance has obscured the moisture results because the shape functions used for numerical solution of the conductances cannot accelerate fast enough to produce an accurate value.

5. DISCUSSION

Figure 6.4 shows that laboratory calibrated EICT moisture content values range around the expected emplacement level of ~ 18.0% at the beginning of the monitoring (Dixon, Campbell, and Hnatiw 1994).

The laboratory calibrations were performed at 1.67 Mg/m^3 whereas the preplaced buffer moisture was ~ 1.73 Mg/m^3 (Dixon, Campbell, and Hnatiw 1994). The higher emplacement density would manifest itself in a higher apparent moisture content but this correction is not insignificant in the range of conditions experienced. This is shown from the density-resistivity relationship which has the same form as the moisture content-resistivity relationship (Strobel 1994a), ie.,

$$\rho = a' + b' exp(-D/c') \tag{5.1}$$

where $a' = 1.42 \times 10^2$ (Ω-m), $b' = 6.74 \times 10^5$ (Ω-m), and $c' = 1.42 \times 10^{-1}$ ($[Mg/m^3]^{-1}$) were computed as above. From Equations 3.1 and 5.1

$$\delta\rho = (b'/c')\exp[-D/c']\delta D$$

and

$$\delta\rho = (b/c)\exp[-M/c]\delta M$$

Hence

$$\delta M/\delta D = (b'/b)(c/c')(\exp[M/c]\exp[-D/c']$$

Substituting the values of b, c, b', and c' into the above using $M = 17.5\%$ and $D = 1.71$ Mg/m^3:

$$\delta M/\delta D = 0.168\ \%/(Mg/m^3)$$

For a difference of 0.08 Mg/m^3, this translates into an apparent moisture content variation of 0.13%.

Fitting the EICT data to the psychrometer data for the *in situ* calibration implies that the psychrometer data is a measurement standard. Alternatively, evaluating the psychrometer results as compared to the EICT measurements helps to understand the performance of the

psychrometers. The trends in both data sets is consistent and this observation is validated by the other results (Strobel 1994b). However, the psychrometer and laboratory calibrated EICT results are offset relative to each other by ~ 10% of the readings. The psychrometer data is higher then expected: averaging 19 to 20% by mass from early in the tests when the expected results should be less then 18%. The consistency in the trends with the EICT results help validate the psychrometer moisture content trends, if not their absolute values. To make them consistent in magnitude they need only be linearly transformed. The fact that the parameters in the calibrated *in situ* relationship are close to those of the calibration curve, differing by $\ll 1\%$ and 13% for α and β respectively, implies that this shift is small. The transformation can be calculated from the calibration curves (above):

$$M = M'(\beta/\beta') + [\alpha - \beta/\beta'\alpha']$$

$$= 0.9776 \times M' - 0.278$$

where M is the corrected moisture content and M' is the calculated psychrometer moisture content. This is an offset of ~ 10% at 18% moisture content: consistent with the observed offset for the psychrometer values.

The expected inflow of moisture from the walls of the borehole is apparent from Figure 6.3 as an increase in moisture at the ends of the plot. The moisture levels computed for boundary will be lower than the actual moisture content because the analysis used nodes placed on the rock-buffer interface. The rock has a lower conductance than the buffer and the fit produced will be influenced by both the buffer and the rock.

The factors having the largest influence on the response of the system appears to be internal since the internal response is significantly greater than that caused by direct moisture inflow. Changes in moisture content of up to 2% in four months has affected all regions of the system. The magnitude of the moisture inflow cannot be directly determined from the EICT readings due to the effect of the rock wall: however, the change in moisture content can give this result. It appears that significant moisture inflows are occurring at the boundary, but, restricted to the outer 0.5 *m* of the borehole.

The result from calibration with laboratory measurements show a similar trend to the results from the *in situ* calibration. They are offset downwards. This consistency in the trend is not surprising since the form of the calibration curves used are the same with only the calibration parameters calculated in a different manner. The results from the laboratory calibration were more consistent with the preplaced moisture of the buffer. The distributed change in the moisture content for 1993 February 6 is displayed in Figure 6.5.

Equation 3.2 assumes the electrical resistivity of the buffer is dominated by the pore water. If this is the case, the results of these tests can be used to deduce a value for the porosity of the *in situ* buffer. That the parameter a in Equation 3.1 is not insignificant suggests there is a major contribution to the resistivity due to the buffer matrix. This would be the contribution due to the clay minerals. Considering the second term in Equation 3.1 to be due to the pore water: since $\phi = \xi\epsilon$ and $c = ln^{-1}(\xi\epsilon)$, then the porosity (void volume/total volume) of the *in situ* buffer is $\phi = \epsilon^{[-1/c]} = 0.652$. This value is high compared to the expected ~ 0.40 (D.

Dixon, personal communication) which could be due to the high clay content of the buffer causing a lower resistivity.

6. CONCLUSIONS

The results show that the EICT method can be used to monitor buffer to produce a quantitative result for moisture distribution. The trend in these results were validated by the psychrometer readings. The EICT and psychrometer moisture values were offset relative to each other; however, independently calibrated EICT moisture values were consistent with the initial conditions of the system. The absolute results for the EICT moisture values are incorrect at the boundary of the system because the electrodes were placed on the buffer-rock interface. The interface is a mathematical discontinuity for the processing model and the conductance of the associated nodes will not be able to determine a correct value at these nodes. However, by presenting the data as a change relative to a reference date, as in Figure 6.5, a change in moisture content can be calculated for this region.

ACKNOWLEDGMENTS

The Canadian Nuclear Fuel Waste Management Program is jointly funded by AECL and Ontario Hydro under the auspices of the CANDU Owners Group.

REFERENCES

Archie, G. 1942. The electrical resistivity log as an aid in determining some reservoir characteristics. Trans. A.I.M.E. 146, 54-62.

Dixon, D., S. Campbell, and D. Hnatiw. 1994. Preplacement quality control and as-placed properties of the buffer materials used in the URL Isothermal Buffer Experiment. Atomic Energy of Canada Limited, Technical Record TR-612, COG-94-35.

Dormuth, K. and P. Gillespie. 1990. Nuclear fuel waste disposal in Canada—the generic research program. Atomic Energy of Canada Limited, Technical Report AECL-10183.

Simmons, G. 1987. Atomic Energy of Canada Limited's Underground Research Laboratory for Nuclear Waste Management. Atomic Energy of Canada Limited, Technical Report AECL-9283.

Strobel, G. 1994a. Measurements of resistive and capacitive properties of a sand/bentonite clay mixture. Atomic Energy of Canada Limited, Technical Report AECL-10668, COG-92-195.

Strobel, G. 1994b. A method for fitting multiple sets of noncoincidental stochastic data. Atomic Energy of Canada Limited, Technical Report TR-450, COG-94-468.

Strobel, G. 1994c. Resistivity-water content relationship of a sand/bentonite clay mixture. Atomic Energy of Canada Limited, Technical Report TR-600, COG-93-90.

robel, G. 1995. An impedance-computed tomographic data acquisition system. Atomic Energy of Canada Limited, Technical report.

an, A. 1995. An appraisal of the usefulness and limitations of commercial thermocouple psychrometers for soil suction potential measurements. Atomic Energy of Canada Limited, Technical Report AECL-11091.

TABLE 6.1:

Laboratory Data Determining Calibration Curve

Moisture Content (%)	Measured Voltage (V)	Point Resistance (Ω)
14.86	4.088	445.58
15.44	3.3586	366.37
15.52	3.6306	396.04
15.99	3.2525	354.79
16.40	3.1088	339.12
16.78	2.8324	308.97
17.60	2.3404	263.98
17.61	2.2778	255.30
17.50	2.420	248.47
17.99	2.3296	254.12
18.07	1.9994	218.10
18.31	2.1644	236.10
18.40	2.0892	227.96
18.57	1.8898	206.15
19.64	1.8238	198.95
19.69	1.7678	192.84
20.33	1.6966	185.07
20.46	1.6642	181.54
21.79	1.6384	175.91
21.73	1.6126	178.72
21.83	1.6696	182.13

TABLE 6.2:

In Situ and Laboratory Calibrated Moisture Contents

Distance from center (m)	Laboratory Calibrated Moisture (%)	Calibrated *in situ* Moisture (%)	Distance from center (m)	Laboratory Calibrated Moisture (%)	Calibrated *in situ* Moisture (%)
-0.611	15.55	17.17	0.113	18.41	19.66
-0.611	15.67	17.27	0.141	18.52	19.75
-0.611	15.43	17.07	0.190	18.59	19.82
-0.566	15.81	17.40	0.239	18.63	19.85
-0.566	15.70	17.30	0.267	18.49	19.73
-0.566	15.67	17.27	0.316	18.33	19.59
-0.522	16.16	17.70	0.359	17.99	19.29
-0.522	16.27	17.79	0.365	17.87	19.19
-0.522	16.17	17.71	0.388	17.85	19.17
-0.494	16.18	17.72	0.394	17.64	18.98
-0.493	16.47	17.97	0.440	16.67	18.14
-0.443	17.16	18.57	0.443	16.61	18.09
-0.440	17.10	18.51	0.493	15.88	17.46
-0.394	17.70	19.04	0.494	15.72	17.32
-0.388	17.67	19.01	0.522	15.58	17.20
-0.365	17.96	19.27	0.522	15.57	17.19
-0.359	17.74	19.07	0.522	15.52	17.14
-0.316	18.21	19.48	0.566	15.12	16.80
-0.267	18.20	19.48	0.566	15.13	16.80
-0.239	18.26	19.53	0.566	15.11	16.79
-0.190	18.14	19.42	0.611	14.88	16.58
-0.141	17.91	19.22	0.611	15.06	16.74
-0.113	17.92	19.23	0.611	15.12	16.80

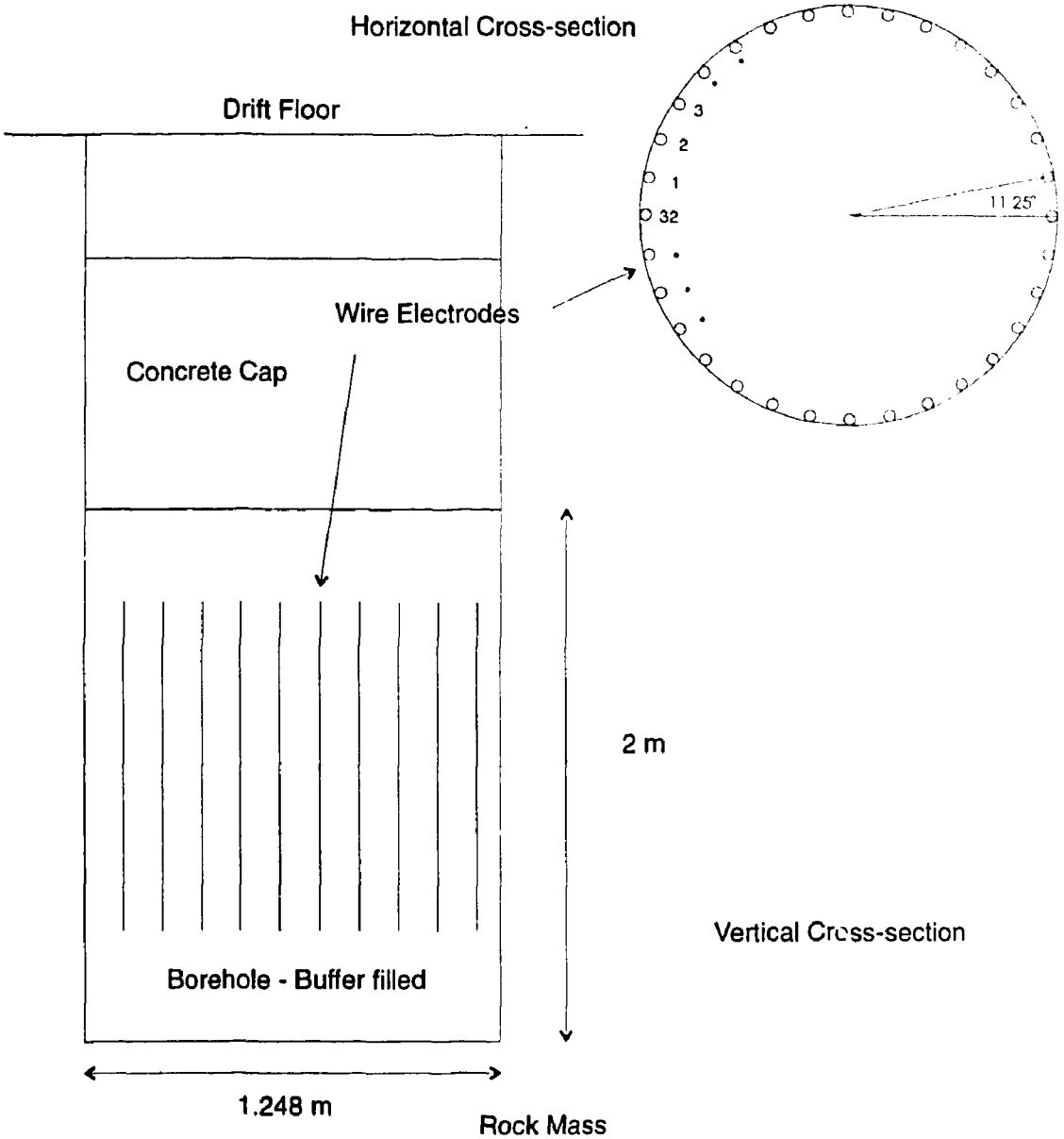

FIGURE 6.1: Apparatus used for the Reported Tests. The electrodes were installed in a borehole in the floor of the drift and selected in pairs for the excitation circuit. Voltages were measured at the other electrodes.

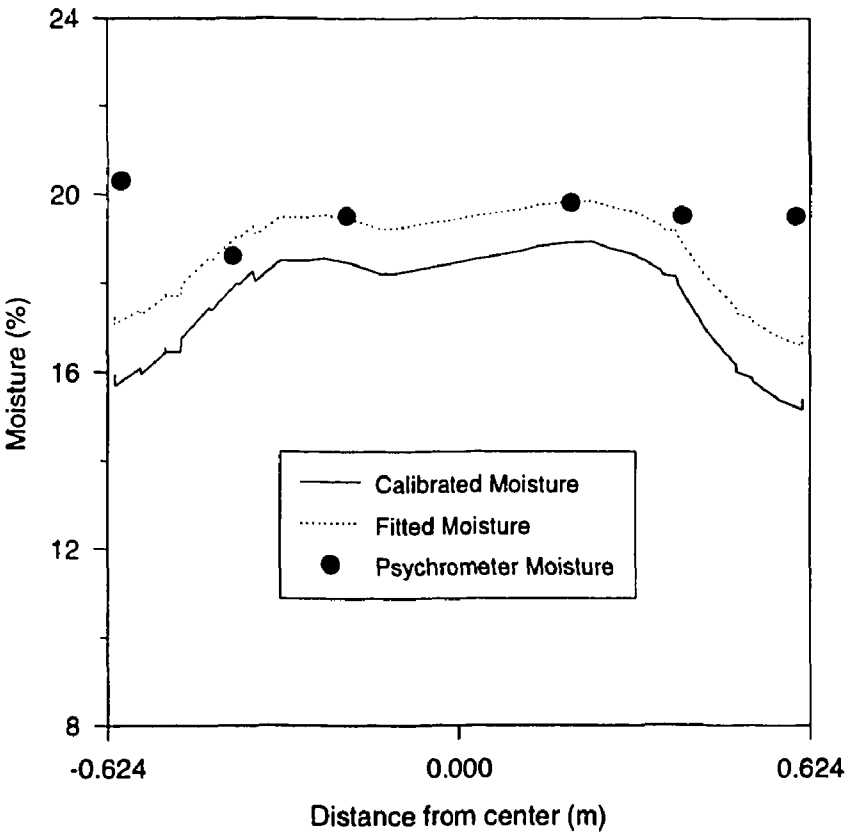

FIGURE 6.2: Plot of Fitted and Laboratory Calibrated Data for 1993 February 6. The conductance data was calibrated using the results of (Strobel 1994c) and, alternatively, fitted according to (Strobel 1994b). The average moisture content is computed from moisture distributions (Dixon, Campbell, and Hnatiw 1994) in the buffer in the $1 - m$ region surrounded by the electrodes. The psychrometer readings were also plotted.

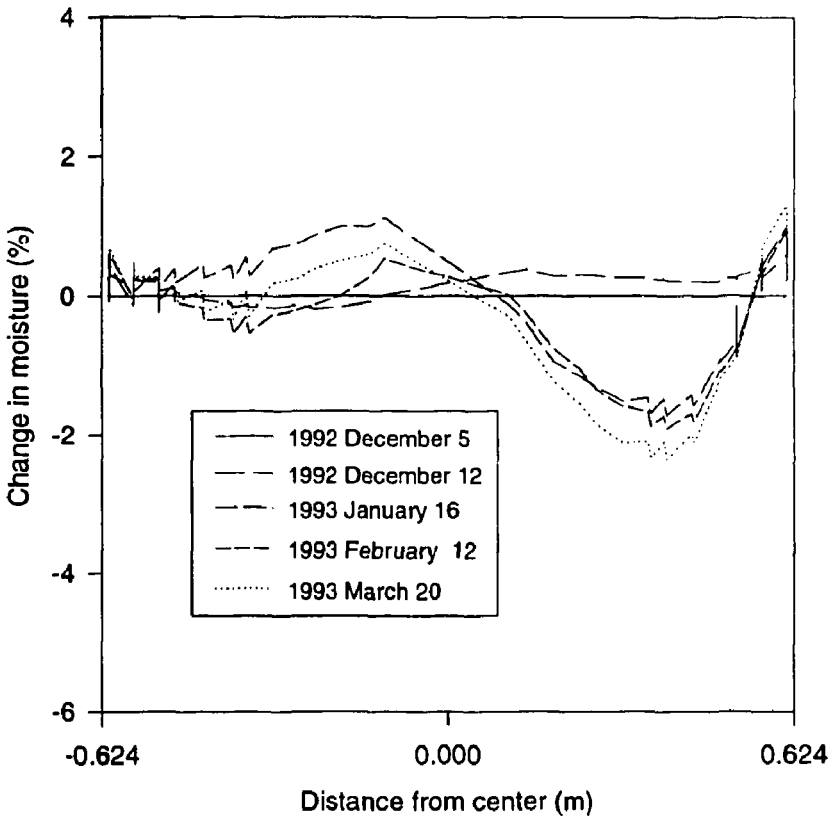

FIGURE 6.3: Change in Moisture Content over Four Months. The moisture content was computed from the calibration curve for measurements and the profiles were plotted for four days over four months. The reference profile used was 1992 December 5.

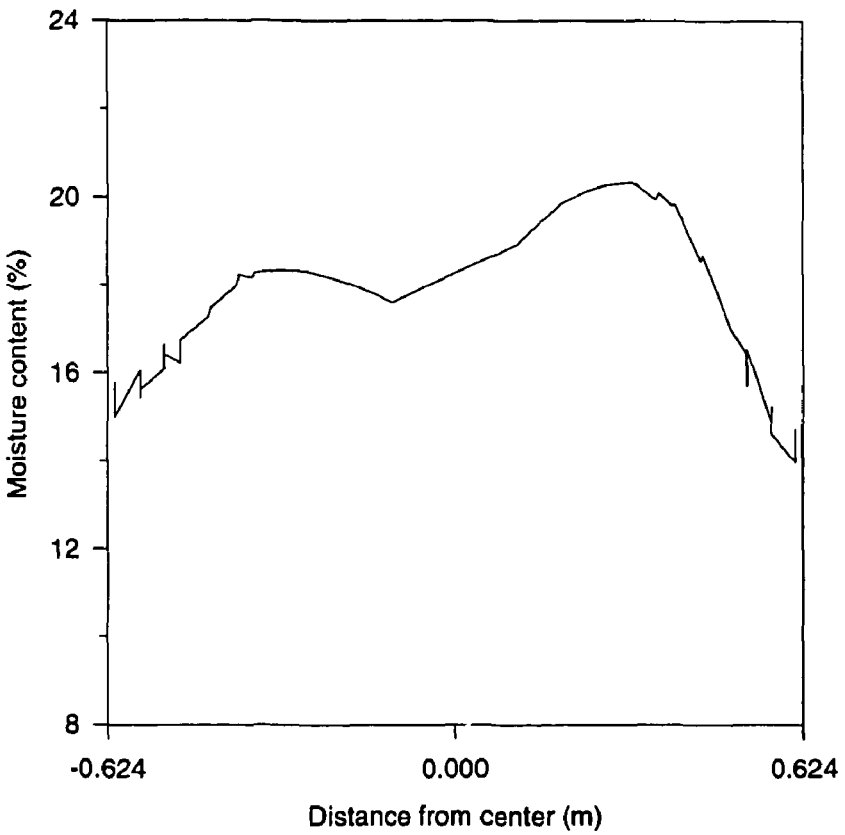

FIGURE 6.4: Laboratory Calibrated Data for 1992 December 5. The conductance data determined from the EICT survey was calibrated using results from the laboratory tests.

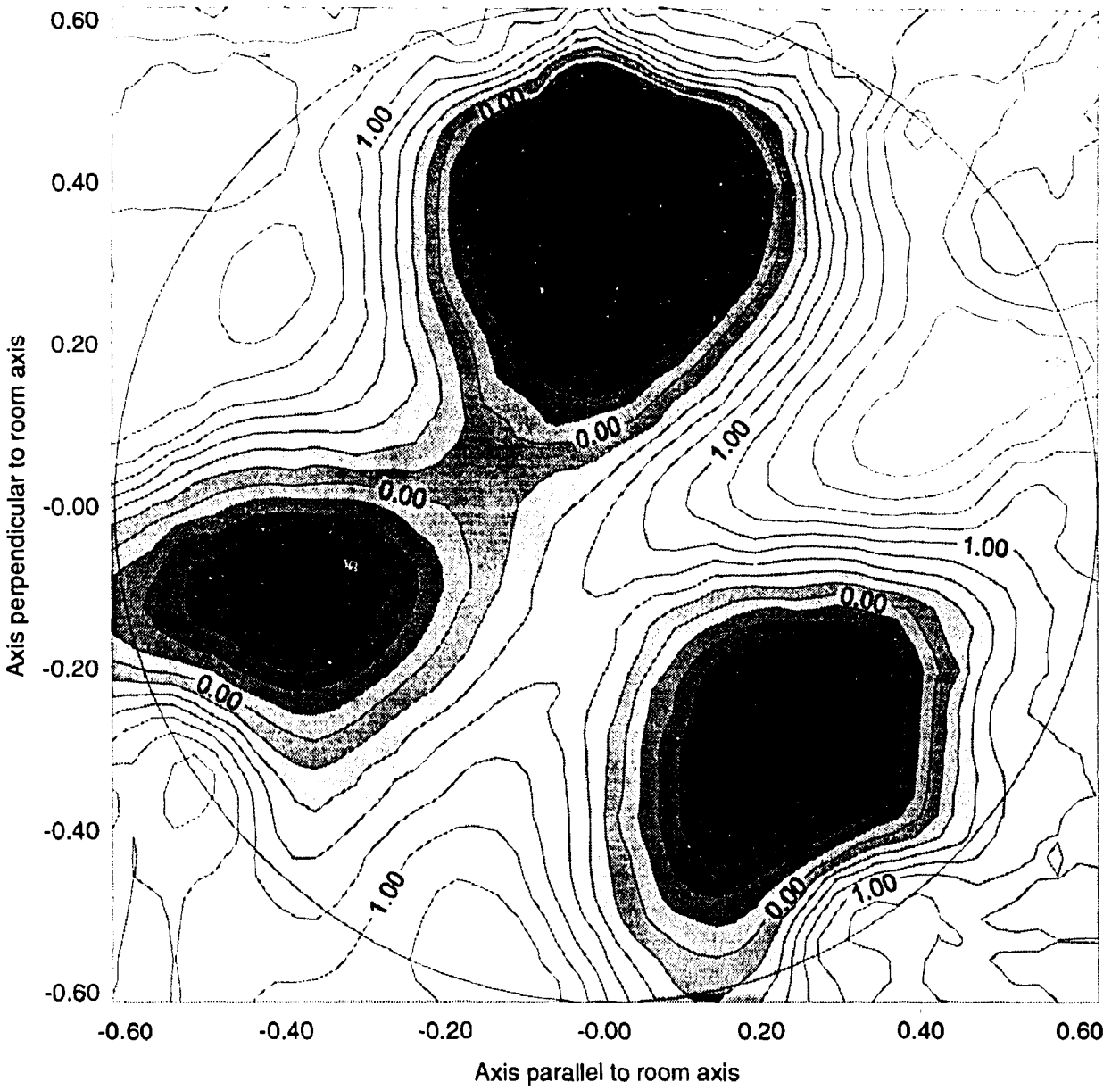

FIGURE 6.5: Moisture Plot from Laboratory Calibrated Conductance Readings. The plot is a distribution of the change in moisture content as of 1993 February 06, relative to 1992 December 05. Units are % moisture content.

Cat. No. / Nº de cat.: CC2-11190E
ISBN 0-660-16274-8
ISSN 0067-0367

To identify individual documents in the series, we have assigned an AECL- number to each. Please refer to the AECL- number when requesting additional copies of this document from

Scientific Document Distribution Office (SDDO)
AECL
Chalk River, Ontario
Canada K0J 1J0

Fax: (613) 584-1745 Tel.: (613) 584-3311
ext. 4623

Price: A

Pour identifier les rapports individuels faisant partie de cette série, nous avons affecté un numéro AECL- à chacun d'eux. Veuillez indiquer le numéro AECL- lorsque vous demandez d'autres exemplaires de ce rapport au

Service de Distribution des documents officiels (SDDO)
EACL
Chalk River (Ontario)
Canada K0J 1J0

Fax: (613) 584-1745 Tél.: (613) 584-3311
poste 4623

Prix: A